This is a repository copy of *Ester hydrolysis: Conditions for acid autocatalysis and a kinetic switch*.

Accepted Manuscript

Ester hydrolysis: Conditions for acid autocatalysis and a kinetic switch

Tamás Bánsági, Annette F. Taylor

Ester hydrolysis: conditions for acid autocatalysis and a kinetic switch

Tamás Bánsági and Annette F. Taylor

Chemical and Biological Engineering, University of Sheffield, S1 3JD

We dedicate this paper to Prof. Ben Feringa on the occasion of the award of the 2016 Tetrahedron Prize and the Nobel Prize in Chemistry.

Abstract

Autocatalysis can be used to obtain a sharp switch in state after a programmable time lag. Here, autocatalysis driven by acid concentration during the dissolution and hydrolysis of solid esters was investigated. In a generic model of the process, conditions were identified for observation of a kinetic switch with the introduction of an inhibitor species, bicarbonate, to delay the onset of autocatalysis. The kinetic profiles from the hydrolysis of two esters, D-gluconic acid δ-lactone and DL-lactide, were examined and evidence for dissolution-limited acid autocatalysis was obtained with lactide.

Keywords: autocatalysis, ester hydrolysis, acid-base catalysis, kinetic modelling
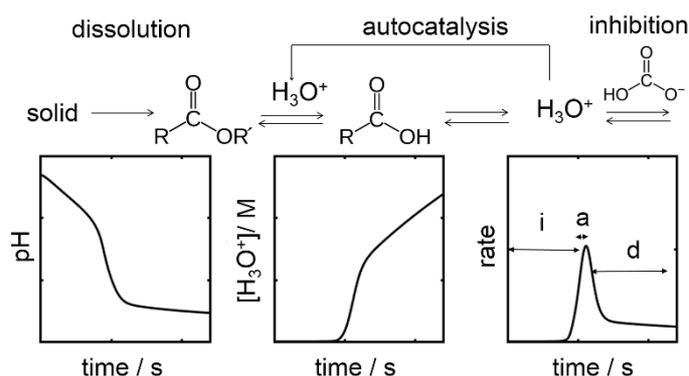
1. Introduction

The term switch in chemistry is typically used to describe a molecule that responds to environmental stimuli, such as light or pH, with a change in conformational state.[1] Alternatively, a kinetic switch might be defined as one in which a chemical reaction sharply switches between a low and high concentration of product. This situation can arise in the presence of autocatalysis, when a product accelerates the rate of reaction.[2]

Autocatalysis plays an important role in diverse processes such as amplification of an enantiomeric species[3,4], template-directed synthesis[5] and activation of trypsinogen by trypsin.[6] In a closed system, autocatalysis often manifests as an exponential increase in product after a time lag. Autocatalytic reactions also have the potential to be maintained in a low conversion state far-from-equilibrium and initiated on-demand. These kinetic switches may be useful when a rapid change in state is desired after a programmable length of time; for example, acid or base production can be coupled to material formation/degradation in coatings, adhesives or drug delivery devices.[7,8] New sources of autocatalysis generating changes in pH are being sought for such applications.[9]

One well know example of acid autocatalysis is ester hydrolysis. In this reaction, the formation of the carboxylic acid product can catalyse the hydrolysis resulting in an increase in reaction rate under non-buffered conditions. In fact, most (if not all) of the examples of autocatalysis by this mechanism take place in heterogeneous environments where other factors play an important role in the observed kinetics.[10,11] In the hydrolytic degradation of polyesters such as poly(lactic acid), the rate acceleration in loss of mass has been attributed to the increasing concentration of terminal carboxylic acid groups.[12] However, rate acceleration with liquid esters was demonstrated to arise by a physical mechanism whereby the product effectively aids in the solubilisation of the reactant.[13]

Here, evidence was examined for acid autocatalysis in the hydrolysis of two solid esters with differing dissolution rates: D-gluconic acid δ-lactone and DL-lactide, the cyclic ester from which poly(lactic acid) can be synthesised. Although the kinetic constants for gluconolactone hydrolysis are well established,[14] surprisingly little exists in the literature on lactide hydrolysis. Hence we examined the conditions for a switch in a generic model designed to capture the main features of the reaction, rather than focussing on detailed, accurate models of the different cases presented experimentally. The addition of an inhibitor species, bicarbonate, that removes the acid, was included in order to delay the onset of autocatalysis. It was found that experimentally, lactide displayed features indicative of dissolution-limited acid autocatalysis whereas the acid catalysis was too weak in the case of gluconolactone for autocatalysis. A general strategy for obtaining kinetic switches in acid in ester hydrolysis is discussed.

2. Kinetic Model

A dissolving sphere model was assumed for the increase in aqueous ester concentration $[R_1COOR_2]$ when solid crystals were added to water:

$$R_1COOR_2(s) \xrightarrow{H_2O} R_1COOR_2(aq) \qquad \frac{d[R_1COOR_2]}{dt} = \frac{SA}{V}k_0 \qquad (1)$$

where SA is the total surface area of the crystals, V is the volume of water and k_0 is the (constant) rate at which the ester is stripped from the solid surface (mol dm^{-2} s^{-1}) which depends on a mass transfer coefficient (sensitive to stirring rate, units of dm s^{-1}) and concentration of solid at the crystal surface (units of mol dm^{-3}). The total surface area is determined from $4\pi r^2 N$ where N is the number of crystals and r is the average crystal radius, r, which decreases linearly in time:

$$\frac{dr}{dt} = -\frac{M_r}{\rho}k_0 \qquad (2)$$

with ρ = the density of the crystals and M_r = the molar mass of the ester. The hydrolysis reaction rate is given by:

$$R_1COOR_2 \xrightarrow{H_2O, H_3O^+} R_1COOH + R_2OH \qquad rate = (k_1 + k_h[H_3O^+])[R_1COOR_2] \qquad (3)$$

where k_1 is the first order rate constant and k_h is the rate constant of the acid catalysed path. The reversibility of this reaction and base catalysis were ignored as they were found to play a negligible role in the kinetic profiles obtained here. The following reversible reactions were included for the dissociation of the carboxylic acid and water:

$$R_1COOH \xrightleftharpoons{H_2O} R_1COO^- + H_3O^+ \qquad rate = k_2[R_1COOH] - k_{2r}[RCOO^-][H_3O^+] \qquad (4)$$

$$2H_2O \xrightleftharpoons{} OH^- + H_3O^+ \qquad rate = k_3 - k_{3r}[OH^-][H_3O^+] \qquad (5)$$
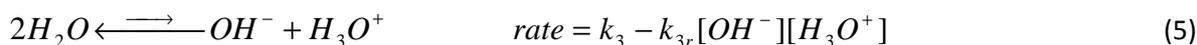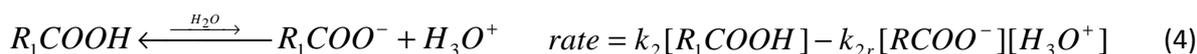
The values of the rate constants, unless otherwise stated, were: $k_0 = 1 \times 10^{-5}$ mol dm^{-2} s^{-1}, $k_1 = 1 \times 10^{-3}$ s^{-1}, $K_{a2} = k_2/k_{2r} = 1.4 \times 10^{-4}$ (lactic acid) and $k_2 = 1 \times 10^3$ s^{-1}, $k_3 = 1 \times 10^{-3}$ M s^{-1}; $k_{3r} = 1 \times 10^{11}$ M^{-1} s^{-1}. The values for reactions (4) and (5) were taken from the literature[15] whereas the values for (3) were chosen in order to best illustrate the different cases discussed below. The density $\rho = 1.2$ g/ ml, $M_r = 144$ g/ mol and average crystal radius $r = 0.1$ mm (values for lactide). The volume of water was 20 ml and N was estimated from the initial mass/average crystal mass = $m/(4/3\pi r^3 \rho)$. All simulations had a starting pH of 7.4.

2.1 Case 1: Dissolution-limited autocatalysis

With no acid catalysis, i.e. $k_h = 0$, the concentration of ester in solution increased as the crystals dissolved (Fig. 1(a), red curve). Complete conversion of solid ester to dissolved ester occurred at 8300 s or 2.3 hours: only the first 400 s are shown here. The dissolved ester hydrolysed producing carboxylic acid and there was a decrease in pH and a corresponding increase in H$_3$O$^+$ (Fig. 1 (b) and (c)). The rate of production of H$_3$O$^+$ increased to a constant value that depended strongly on the value of K_{a2} (Fig. 1(d), red curve).

When acid catalysis was included, a sharper drop in pH and rapid increase in the acid concentration was observed (Fig. 1 dashed lines). However, the dissolved ester concentration then rapidly decreased and the rate of acid production fell. Thus there were two processes evident in the acid profile: the first corresponded to a rapid growth from autocatalysis and the second a slow growth when the hydrolysis was limited by the rate of dissolution of ester.
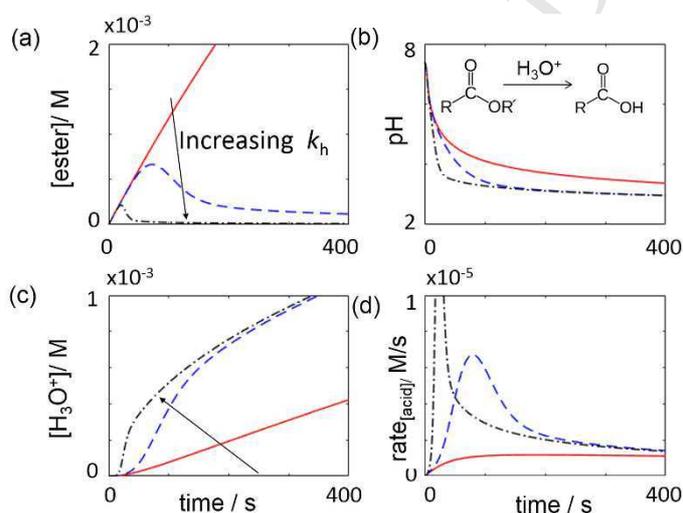
Figure 1. Dissolution-limited autocatalysis in the simulations with mass of solid ester, m = 0.1 g. The time profiles show the (a) concentration of dissolved ester (b) pH (c) concentration of H$_3$O$^+$ and (d) rate of production of H$_3$O$^+$. The value of k_h, was increased (illustrated by the arrow) from 0 (red, solid line) to 10 M^{-1} s^{-1} (blue dashed line) and 20 M^{-1} s^{-1} (black, dash-dot)

2.2 Case 2: Removal of inhibitor, no acid catalysis

In order to delay the onset of the acid (H_3O^+) production, an inhibitor species can be introduced. A simple inhibitor that can be used in experiments with acid is bicarbonate. The rates of reactions and equilibria involving bicarbonate, carbonic acid and carbonate are well established.[16] For the pH range explored here, the behaviour can be accounted for by including the following reversible reaction in the model:

$$CO_2 \xleftrightarrow{\quad H_2O \quad} HCO_3^- + H_3O^+ \qquad\qquad rate = k_4[CO_2] - k_{4r}[HCO_3^-][H_3O^+] \qquad (6)$$
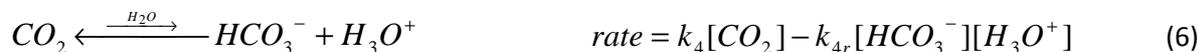
where $[CO_2]$ is the dissolved carbon dioxide concentration, $k_4 = 0.037$ s^{-1} and $k_{4r} = 7.9 \times 10^4$ M^{-1} s^{-1}. The pKa of this equilibrium is 6.3.

The simulations in Figure 2 show the ester dissolution and hydrolysis with inclusion of a HCO_3^- / CO_2 buffer and no acid catalysis ($k_h = 0$). The concentration of aqueous ester was unaffected by the buffer (Fig. 2(a), bold). The bicarbonate removed the acid produced from the ester hydrolysis until its level fell sufficiently (Fig. 2(a)) then there was a sharp drop in pH (Fig. 2(b)) and the concentration of acid (H_3O^+) started to increase linearly in time (Fig. 2(c)). The rate of acid production jumped to a higher value after the time lag set by the initial strength of the buffer (Fig. (2(d)).
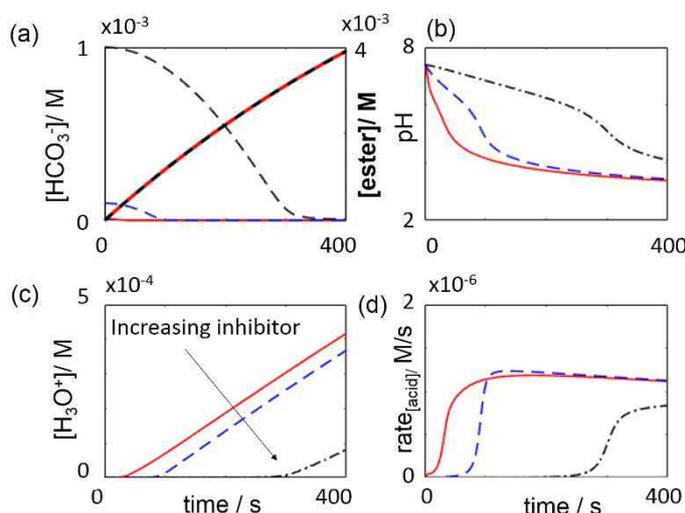

Figure 2. Removal of inhibitor, HCO_3^-, with no acid catalysis and mass of ester, m = 0.1 g. The time profiles show the (a) concentration of bicarbonate and ester (bold) (b) pH (c) concentration of H_3O^+ and (d) rate of production of H_3O^+. The initial concentration of bicarbonate $[HCO_3^-]_0 = 1 \times 10^{-5}$ M (red), 1×10^{-4} M (blue dashed) and 1×10^{-3} M (black, dash dot) and the initial $[CO_2]_0 = [H_3O^+]_0[HCO_3^-]_0/K_{a4}$.

2.3 Case 3. Combined autocatalysis and inhibition

With both acid catalysis and inhibition through HCO_3^-/CO_2 included, the dissolution-limited autocatalysis occurred after a time delay during which the buffer was consumed. For a low initial mass, only a modest increase in rate was observed (Fig. 3(a)). As the mass was increased, the time delay decreased and a sharper increase in acid occurred before it fell to a constant value limited by the rate of dissolution (Fig. 3(c) – (e)).
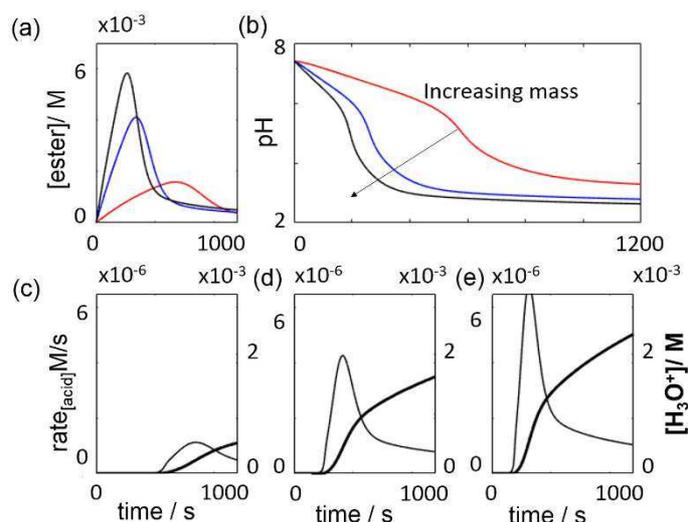
Figure 3. The appearance of autocatalysis and removal of inhibitor with increasing mass of ester where k_h =18 M^{-1} s^{-1} and $[HCO_3^-]$ =1 x 10^{-3} M and $[CO_2]$= 9 x 10^{-5} M. The time profile of (a) dissolved ester (b) pH; initial mass m = 0.03 g (red), 0.13 g (blue,), 0.23 g (black) and (c) – (e) rate (thin line, left axis) and acid (bold line, right axis) where (c) m = 0.03 g (d) m = 0.13 g and (e) m = 0.23 g.

The three cases with slow dissolution are compared in Figure 4 in which the decrease of solid ester (upper plots) and the net rate of change of aqueous ester (lower plots) in time are shown. Neither increasing k_h nor the concentration of inhibitor affected the rate of dissolution of solid ester (cases 1 and 2). This only increased with the initial mass of solid (case 3), resulting in the larger rate of production of acid observed in Figure 3(c). The autocatalytic process manifests clearly in the rate of change of aqueous ester. The net rate rapidly changes from positive (dissolution) to negative (autocatalytic hydrolysis) until the concentration of ester falls sufficiently so that the two processes balance (case 1). Hence the slow dissolution prevents the rapid and complete conversion of reactant to product. With no autocatalysis, the net rate remains positive (case 2), and there is no acceleration in the rate of removal of ester.
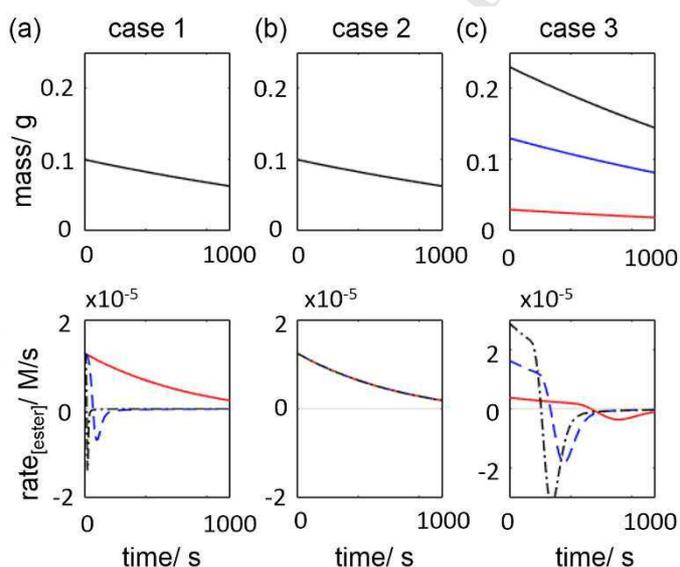

Figure 4. Slow dissolution compared to ester hydrolysis: comparison of the decrease in mass of solid ester and the net rate of change of aqueous ester in the three cases (a) with autocatalysis (k_h = 0 (red, solid line), 10 M^{-1} s^{-1} (blue dashed line) and 20 M^{-1} s^{-1} (black,

dash-dot); all three curves overlap in upper plot) (b) with inhibitor ($[HCO_3^-]_0 = 1 \times 10^{-5}$ M (red), 1×10^{-4} M (blue dashed) and 1×10^{-3} M (black, dash dot); all three curves overlap in both plots) (c) both autocatalysis and inhibitor (initial mass m = 0.03 g (red), 0.13 g (blue,), 0.23 g (black)).

If the dissolution was fast compared to the hydrolysis, then all the solid ester dissolved before significant reaction took place (Fig. 5 (a) and (b)). Then the reaction was dominated by the first order hydrolysis process if acid catalysis, k_h, was weak (Fig. 5(a) and (c)). If the acid catalysis was sufficiently strong, there was an acceleration in the rate of removal of dissolved ester until it was completely consumed and the corresponding sigmoidal production of acid associated with autocatalysis was evident (Fig. 5 (b) and (d)). In both cases, the production of acid occurred after a time lag associated with the removal of bicarbonate.
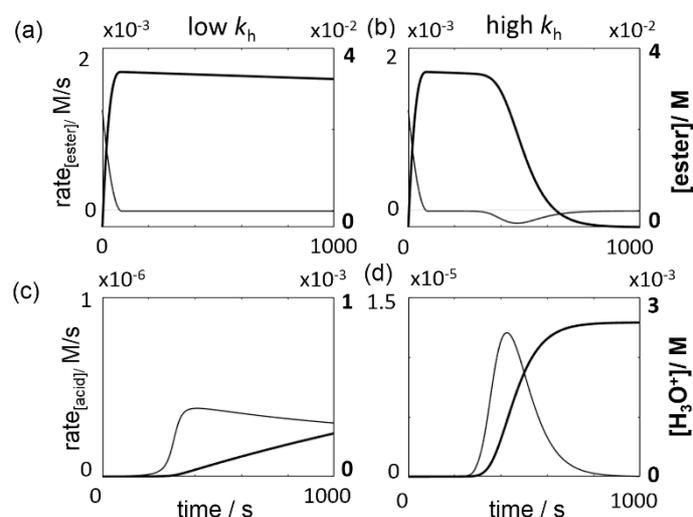

Figure 5. Fast dissolution compared to ester hydrolysis with $k_0 = 1 \times 10^{-3}$ mol dm^{-2} s^{-1} and $k_1 = 5 \times 10^{-4}$ s^{-1} and weak and strong acid catalysis: k_h=0.01 M^{-1} s^{-1} in (a) and (c) and $k_h = 5$ M^{-1} s^{-1} in (b) and (d). The initial mass of ester was m = 0.1 g and $[HCO_3^-]$ =1 $\times 10^{-3}$ M and $[CO_2]$= 9 $\times 10^{-5}$ M.

3. Experimental Results

In the simulations it was established how the slow dissolution can limit the rapid growth in acid and the sigmoidal profile expected from the presence of acid autocatalysis. In the case of fast dissolution, the acid catalysis has to be sufficiently strong compared to the first order hydrolysis in order for autocatalysis to be observed.

In experiments, two solid esters, D-gluconic acid δ-lactone and DL-lactide, with different dissolution rates were tested for evidence of autocatalysis. The same number of moles of solid ester crystals were added to 20 ml of bicarbonate buffer (1 $\times 10^{-3}$ M and pH = 7.5) in order to compare the two systems. The pH time profiles, rate and acid concentration in time are shown in Figure 6. DL-lactide dissolved slowly; complete dissolution of 0.116 g took approximately 1.5 hours. After 300 s, a sharp drop in pH was observed. There was a sharp production of acid and peak in the rate of production of acid: evidence of the autocatalytic process that is limited by the rate of delivery of ester to solution. In the case of gluconolactone, dissolution took seconds. Around 250 s a sharp drop in pH was observed,

this was followed by a slow conversion of ester to acid, with no evidence of the autocatalytic process.
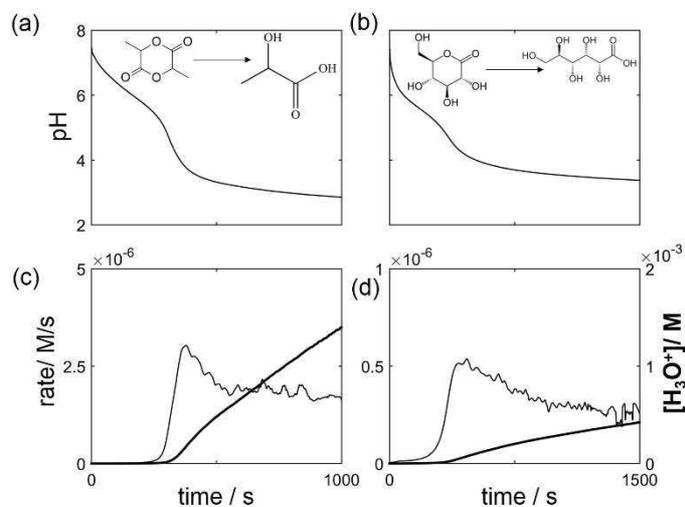
Figure 6. Dissolution and hydrolysis of ester crystals in experiments with bicarbonate/carbon dioxide buffer; $[HCO_3^-]$ = 1 x 10^{-3} M and initial pH = 7.5. DL-lactide, m = 0.116 g in (a), (c), and gluconolactone, m = 0.09 g in (b), (d). In (a) and (b): pH-time profiles. In (c) and (d): concentration of acid (bold lines, left axis) and rate of production of acid (thin lines left axis).

In order to further investigate the dissolution-limited autocatalysis process, different masses of lactide were added to 20 ml of buffer (Fig. 7). The lag time was found to depend on the mass added. With m = 0.03 g, there was only a small peak in the rate of production of acid and this increased with increasing mass. In all cases, the rate then fell to a constant value. With changing mass in the gluconolactone experiments, the form of the acid profile did not change.
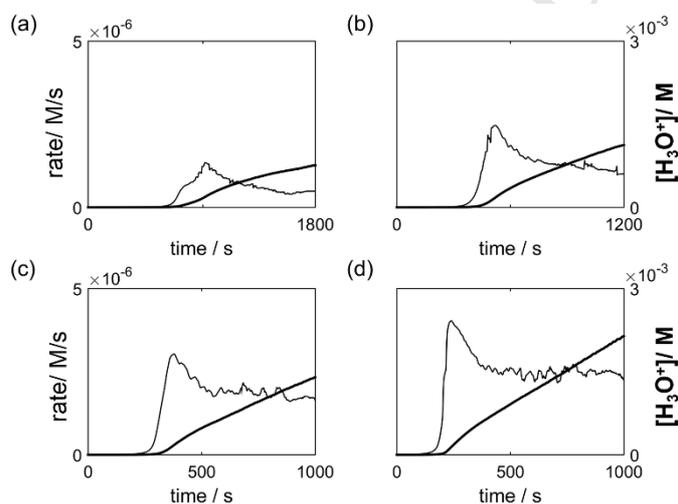
Figure 7. The dissolution and hydrolysis of different masses of DL-lactide in experiments with 20 ml of bicarbonate/carbon dioxide buffer with $[HCO_3^-]$ = 1 x 10^{-3} M and initial pH = 7.5 where m = (a) 0.029 g, (b) 0.058 g, (c) 0.116 g and (d) 0.232 g: concentration of acid (bold lines, left axis) and rate of production of acid (thin lines, left axis).

The simple model appears to explain the experimentally observed cases well. We note that in the case of lactide, two lactic acid molecules are produced; and the reversibility of the ester hydrolysis is likely important in the case of gluconolactone. However we found that

these features did not play a role in the general dynamics illustrated here. With gluconolactone, the first order hydrolysis is more significant than the acid catalysis at these pH values. The literature values[14] of $k_1 = 4.3 \times 10^{-5}$ s^{-1} and $k_h = 3 \times 10^{-2}$ M^{-1} s^{-1} are similar to those used in Figure 4 thereby affirming that the acid catalysis is likely too weak to be able to initiate autocatalysis in this system. Although poly(lactic acid) hydrolysis has also been extensively studied, there was very little in the literature with regards to lactide, and no rate constants for the acid-base catalysed hydrolysis were available to compare with the simulations. Therefore a more detailed study is required to better quantify the hydrolysis process in this case. However the experimental results shown in Figure 7 compare well with those shown in Figure 3 with $k_1 = 1 \times 10^{-3}$ s^{-1} and $k_h = 18$ M^{-1} s^{-1}.

In addition, it was demonstrated how the bicarbonate/carbon dioxide buffer can be used in experiments to effectively delay the onset of acid production and autocatalysis in ester hydrolysis with precise control over the time lag. A kinetic switch is here defined as one in which rapid production of a species, acid, is observed after a programmable length of time. It is well understood that removal of an inhibitor without autocatalysis can result in rapid production of a species after a time lag.[17,18] However there is an important difference in these two cases. With autocatalysis, both the rate of production of acid and the rate of removal of substrate, aqueous ester, accelerate in time. In the presence of just inhibition, there is no increase in the rate of removal of ester as the reaction progresses. Many of the more complex, emergent features associated with autocatalysis and exploited by natural systems are not possible under these conditions. Nevertheless, inhibition alone may still be beneficial for time-lapse applications such as in adhesives.

In closed reactors, the low conversion state cannot be maintained indefinitely and the system moves inexorably towards the high product state. A low conversion state can be maintained under open conditions when the production of acid is counterbalanced by outflow of acid.[19] Then a kinetic switch that responds to changes substrate is possible. For these open systems, conditions could be sought in which the rate of hydrolysis is sufficiently slow to allow the ester to fully dissolve, for example under neutral conditions, before significant changes in pH occur.

A number of systems exploiting kinetic switches have been used recently to drive polymerisation/polymer degradation processes or self-assembly.[20-22] Many of these examples involved harsh inorganic, redox reactions that limit their eventual application and new sources of autocatalysis are being sought.[23] Experimentally, it remains a challenge to find evidence of autocatalysis with an ester that dissolves quickly and displays strong acid catalysis such that a true autocatalytic switch in pH can be obtained for such applications.

4. Conclusions

In conclusion, a model incorporating dissolution of solid ester crystals and hydrolysis was used in order to explore the parameters for which autocatalysis and a kinetic switch might be observed. Experimentally two esters with different rates of dissolution were explored: D-gluconic acid δ-lactone and DL-lactide. It was demonstrated that the acid catalysis was too weak with gluconolactone for autocatalysis however lactide showed evidence of dissolution-limited autocatalysis. In addition, it was found that the onset of acid production can be delayed by use of bicarbonate as inhibitor, resulting in an effective means of programming the time delay of acid autocatalysis with ester hydrolysis.

5. Experimental Section

Reagents: DL–lactide (Alfa Aesar, 99%), D-gluconic acid δ-lactone (Sigma, >99%) and sodium bicarbonate (Sigma) were used without further purification. Sodium bicarbonate/carbon dioxide solutions were prepared with a sodium bicarbonate concentration of 1×10^{-3} mol/dm^3 in deionized water (Milli-Q, 18.2 MΩcm) exposed to air until the pH stabilised at 7.5.

Procedure: Requisite amounts of DL–lactide or D-gluconic acid δ-lactone were added to 20 ml of the bicarbonate solution and the pH of the open-to-air mixtures was recorded using a Hanna HI-1131B combination pH electrode connected to a Pico Technology DrDAQ data logger with all samples stirred at the same rate using a magnetic stirrer bar rotating at a rate of 400 rpm. Experiments were carried out at 22±1 ℃. Each experiment was performed five times and the resulting pH-time profiles averaged to obtain the plots displayed in the figures. The rate data was noisy at low pH as small changes in the signal result in large fluctuations in the slope of the calculated acid concentration in time. Average crystal sizes and dissolution rates were estimated from optical imaging of the samples before and during experiments. Data processing and simulations were performed in MATLAB®.

Acknowledgements

References

1. Feringa, B. L.; Van Delden, R. A.; Koumura, N.; Geertsema, E. M. *Chemical Reviews* **2000,** *100*, 1789-1816.
2. Bissette, A. J.; Fletcher, S. P. *Angewandte Chemie - International Edition* **2013,** *52*, 12800-12826.
3. Satyanarayana, T.; Kagan, H. B. *Tetrahedron* **2007,** *63*, 6415-6422.
4. Blackmond, D. G. *Tetrahedron Asymmetry* **2010,** *21*, 1630-1634.
5. Dela Amo, V.; Philp, D. *Chemistry - A European Journal* **2010,** *16*, 13304-13318.
6. Semenov, S. N.; Wong, A. S. Y.; van der Made, R. M.; Postma, S. G. J.; Groen, J.; van Roekel, H. W. H.; de Greef, T. F. A.; Huck, W. T. S. *Nat. Chem.* **2015,** *7*, 160-165.
7. Heuser, T.; Weyandt, E.; Walther, A. *Angewandte Chemie - International Edition* **2015,** *54*, 13258-13262.
8. Jee, E.; Bánsági, T., Jr.; Taylor, A. F.; Pojman, J. A. *Angewandte Chemie - International Edition* **2016,** *55*, 2127-2131.
9. Donlon, L.; Novakovic, K. *Chemical Communications* **2014,** *50*, 15506-15508.
10. Ford Versypt, A. N.; Pack, D. W.; Braatz, R. D. *J. Controlled Release* **2013,** *165*, 29-37.
11. Gleadall, A.; Pan, J.; Kruft, M. A.; Kellomäki, M. *Acta Biomaterialia* **2014,** *10*, 2223-2232.
12. Siparsky, G. L.; Voorhees, K. J.; Miao, F. *Journal of Environmental Polymer Degradation* **1998,** *6*, 31-41.
13. Tixier, J.; Pimienta, V.; Buhse, T.; Lavabre, D.; Nagarajan, R.; Micheau, J. C. *Colloids and Surfaces A: Physicochemical and Engineering Aspects* **2000,** *167*, 131-142.
14. Pocker, Y.; Green, E. *J. Am. Chem. Soc.* **1973,** *95*, 113-119.
15. Eigen, M. *Angew. Chem., Int. Ed. Engl* **1964,** *3*, 1-19.
16. Wang, X.; Conway, W.; Burns, R.; McCann, N.; Maeder, M. *J. Phys. Chem. A* **2010,** *114*, 1734-1740.
17. Horváth, A. K.; Nagypál, I. *ChemPhysChem* **2015,** *16*, 588-594.

18. Lente, G.; Bazsa, G.; Fábián, I. *New Journal of Chemistry* **2007,** *31*, 1707.
19. Hu, G.; Pojman, J. A.; Scott, S. K.; Wrobel, M. M.; Taylor, A. F. *J. Phys. Chem. B* **2010,** *114*, 14059-14063.
20. Lagzi, I.; Kowalczyk, B.; Wang, D.; Grzybowski, B. A. *Angew. Chem.* **2010,** *122*, 8798-8801.
21. Hu, G.; Pojman, J. A.; Bounds, C.; Taylor, A. F. *J. Polym. Sci. Part A: Polym. Chem.* **2010,** *48*, 2955-2959.
22. Yashin, V. V.; Suzuki, S.; Yoshida, R.; Balazs, A. C. *J. Mater. Chem.* **2012,** *22*, 13625-13636.
23. Postma, S. G. J.; Vialshin, I. N.; Gerritsen, C. Y.; Bao, M.; Huck, W. T. S. *Angewandte Chemie - International Edition* **2017,** *56*, 1794-1798.